11th U.S. National Congress on Computational Mechanics

Topology Optimization using Phase Field Method and Polygonal Finite Elements

Arun Lal Gain, **Glaucio H. Paulino**

Department of Civil and Environmental Engineering
University of Illinois at Urbana-Champaign

Motivation

- Implicit function method such as level-set function, although attractive, require periodic reinitializations to maintain signed distance characteristics for numerical convergence.

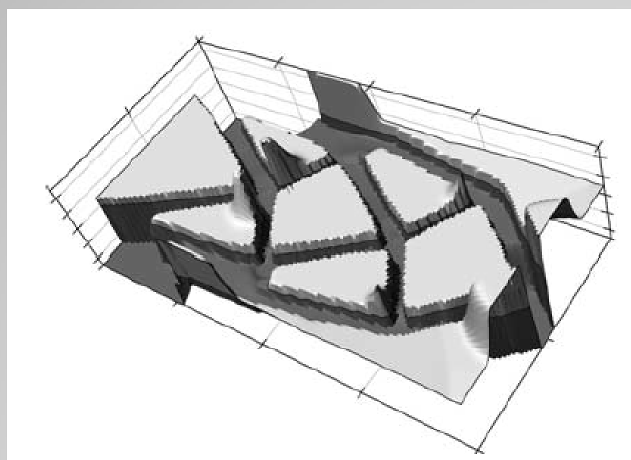

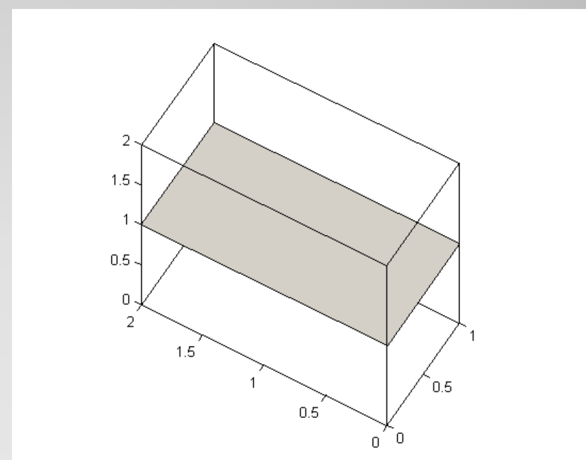

- Reinitializations often performed heuristically.
- Phase field method doesn't require any reinitialization.

Allaire G. and Jouve F. (2004) Structural optimization using sensitivity analysis and a level-set method. Journal of Computational Physics, 194: 363-393

Motivation

- Traditionally uniform grids are used for topology optimization which suffer from numerical anomalies such as checkerboard patterns and one-node connections.
- Constrained geometry of structured grids can bias the orientation of the members, leading to mesh dependent, sub-optimal designs.

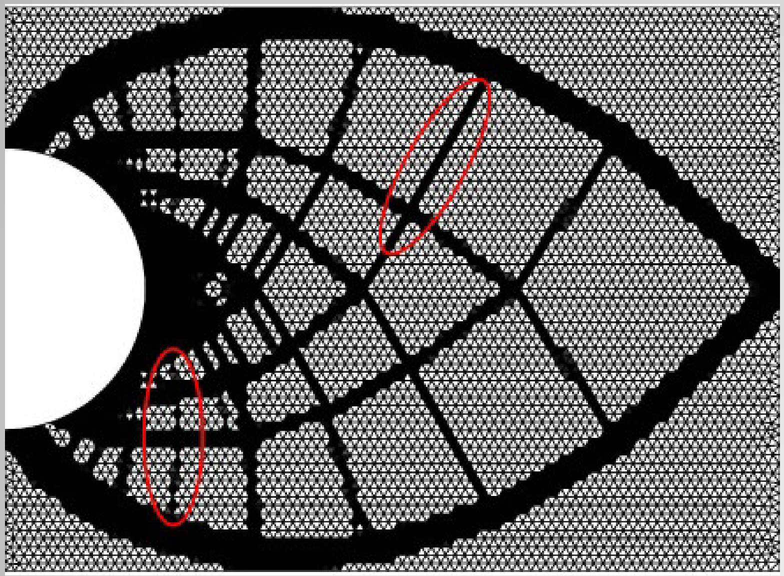

T6 elements

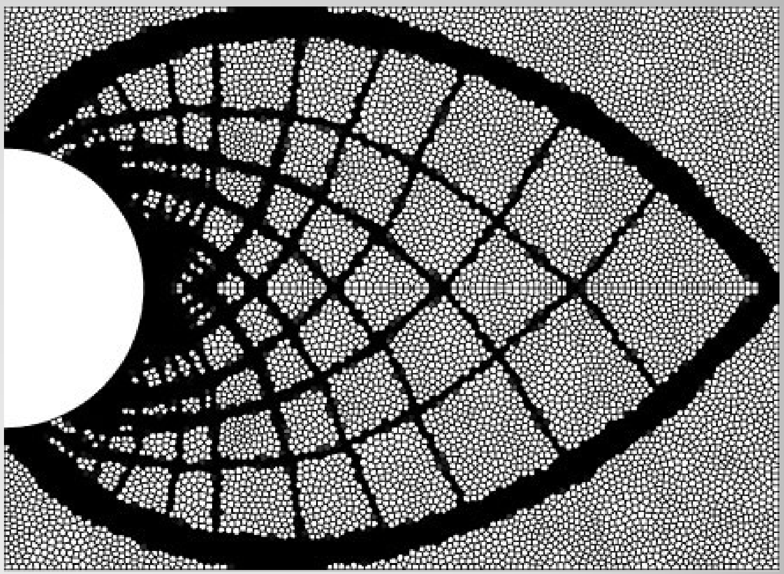

Polygonal elements

Talischi C., Paulino G. H., Pereira A., and Menezes I. F. M. (2010) Polygonal finite elements for topology optimization: A unifying paradigm. International Journal for Numerical Methods in Engineering, 82: 671-698

Motivation

- Explore general and curved domains rather than the traditional Cartesian domains (box-type) that have been extensively used for topology optimization.

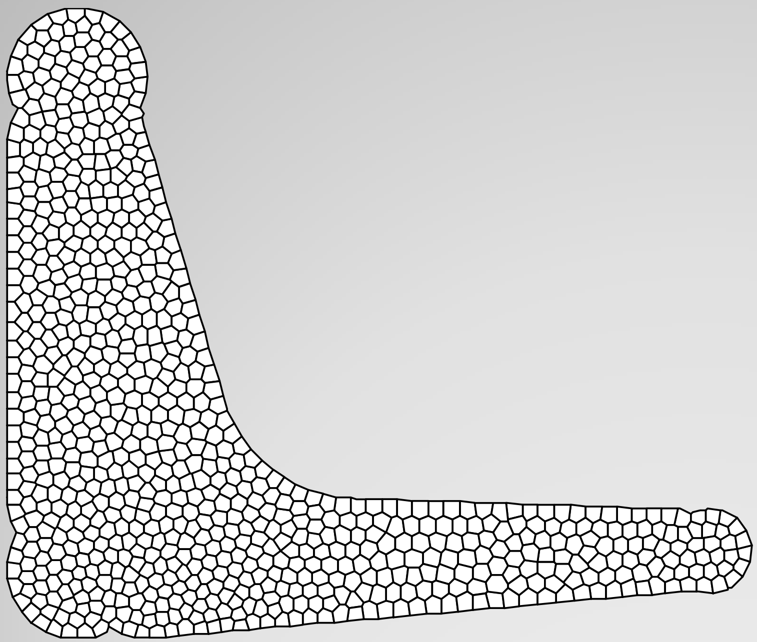

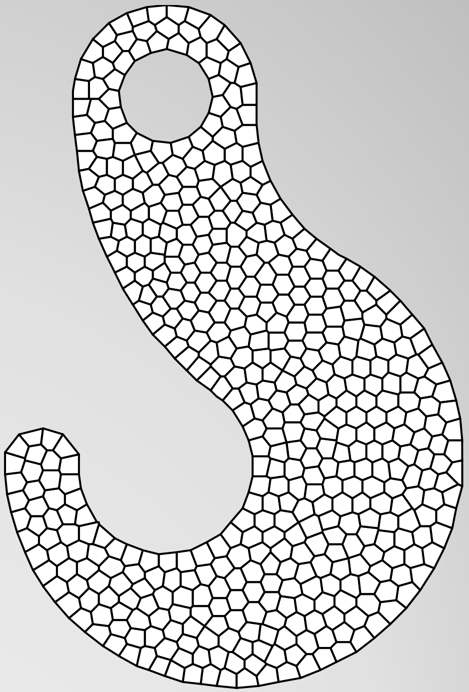

Contents

- Motivation
- Introduction
  - Polygonal Finite Elements
  - Phase Field Method
- Centroidal Voronoi Tessellation (CVT) based finite volume method
- Implementation Flow Chart
- Numerical Examples
- Summary & Conclusions
- Future Extensions

Problem description

- <u>Isotropic linear elastic system:</u>

$$\begin{aligned} -\nabla \cdot (\boldsymbol{A\varepsilon}) &= \boldsymbol{f} && \text{in } \Omega \\ \boldsymbol{u} &= \boldsymbol{0} && \text{on } \Gamma_D \\ (\boldsymbol{A\varepsilon}) \cdot \boldsymbol{n} &= \boldsymbol{g} && \text{on } \Gamma_N \end{aligned}$$

- <u>Objective:</u>

$$\inf_{\Omega} L(\Omega) = \left(J(\Omega) + \lambda P(\Omega) \right)$$

$$J(\Omega) = \int_{\Omega} \boldsymbol{f} \cdot \boldsymbol{u} \, \mathrm{dx} + \int_{\Gamma_N} \boldsymbol{g} \cdot \boldsymbol{u} \, \mathrm{ds}, \qquad \text{Compliance}$$

$$P(\Omega) = \int_{\Omega} \mathrm{dx}, \qquad \text{Volume}$$

Polygonal finite elements

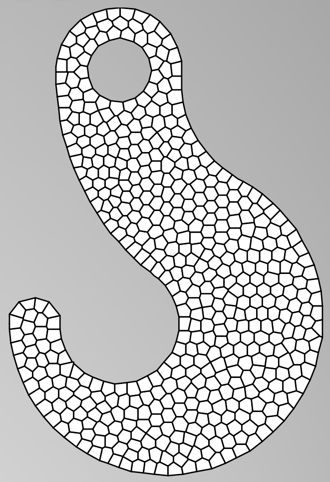

Simple approach to discretize complex geometries using polygonal/polyhedral meshes

Finite element space of polygonal elements is constructed using natural neighbor scheme based Laplace interpolants

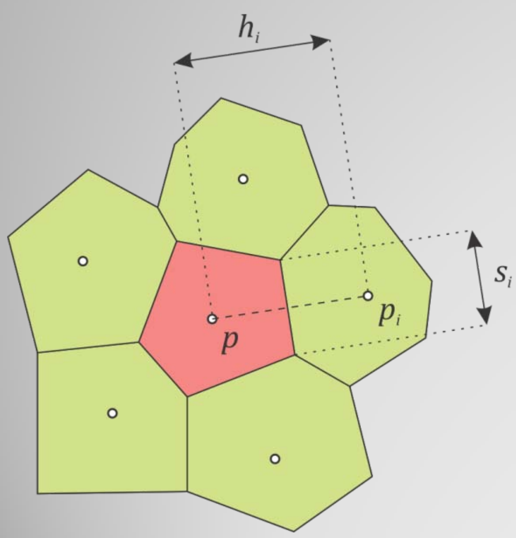

$$N_i(\mathbf{x}) = \frac{\alpha_i(\mathbf{x})}{\sum_{P} \alpha_j(\mathbf{x})}, \qquad \alpha_i(\mathbf{x}) = \frac{s_i(\mathbf{x})}{h_i(\mathbf{x})}, \qquad \mathbf{x} \in \Re^2$$

where, $P = \{p_1, p_2, \dots, p_n\}$

$$0 \le N_i(\mathbf{x}) \le 1, \qquad N_i(\mathbf{x}_j) = \delta_{ij}, \qquad \sum_{P} N_i(\mathbf{x}) = 1$$

$$\sum_{P} \mathbf{x}_i N_i(\mathbf{x}) = \mathbf{x}$$

Sukumar N. and Tabarraei A. (2004) Conforming polygonal finite elements. International Journal of Numerical Methods in Engineering, 61(12): 2045-2066

Phase field method

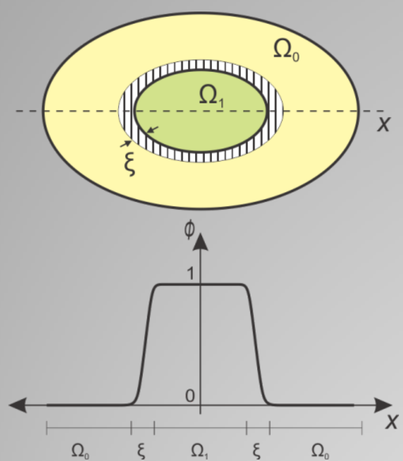

$$\phi = 1 \qquad \boldsymbol{x} \in \Omega_1,$$
$$0 < \phi < 1 \qquad \boldsymbol{x} \in \xi,$$
$$\phi = 0 \qquad \boldsymbol{x} \in \Omega_0,$$

Diffuse interface

$$\boldsymbol{A}^*(\phi) = \begin{cases} \boldsymbol{A} & \boldsymbol{x} \in \Omega_1, \\ k(\phi)\boldsymbol{A} & \boldsymbol{x} \in \xi, \\ k_{\min}\boldsymbol{A} & \boldsymbol{x} \in \Omega_0, \end{cases}$$

<u>Allen-Cahn equation:</u> $$\frac{\partial \phi}{\partial t} = \kappa \nabla^2 \phi - f'(\phi)$$ with $\frac{\partial \phi}{\partial \boldsymbol{n}} = 0$ on ∂D

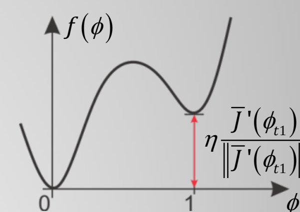

where, $f(0) = 0, \quad f(1) = \eta \frac{\bar{J}'(\phi_{t1})}{\left\| \bar{J}'(\phi_{t1}) \right\|}, \quad f'(0) = f'(1) = 0$

$$\frac{\partial \phi}{\partial t} = \kappa \nabla^2 \phi + \phi(1-\phi)\left[\phi - \frac{1}{2} - 30\eta \frac{\bar{J}'(\phi_{t1})}{\left\| \bar{J}'(\phi_{t1}) \right\|}\phi(1-\phi)\right]$$

Takezawa A., Nishiwaki S., and Kitamura M. (2010) Shape and topology optimization based on the phase field method and sensitivity analysis. Journal of Computational Physics, 229: 2697-2718

Centroidal Voronoi Tessellation (CVT) based finite volume method

Allen-Cahn equation:

$$\frac{\partial \phi}{\partial t} = \kappa \nabla^2 \phi - f'(\phi)$$

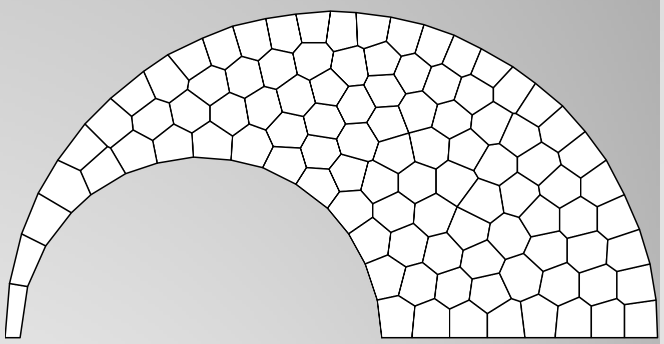

Integral form:

$$\int_{t,\Omega} \frac{\partial \phi}{\partial t} \, d\Omega \, dt = \int_{t,\Omega} \kappa \nabla^2 \phi \, d\Omega \, dt - \int_{t,\Omega} f'(\phi) \, d\Omega \, dt$$

$$\int_{t,\Omega} \frac{\partial \phi}{\partial t} \, d\Omega \, dt = \int_{t,\Gamma} \kappa \boldsymbol{\nabla} \phi \cdot \boldsymbol{n} \, d\Gamma \, dt - \int_{t,\Omega} f'(\phi) \, d\Omega \, dt$$

Vasconcellos J. F. V. and Maliska C. R. (2004) A finite-volume method based on voronoi discretization for fluid flow problems. Numerical Heat Transfer, Part B, 45: 319-342

CVT based finite volume method

Integral form:

$$\int_{t,\Omega} \frac{\partial \phi}{\partial t} d\Omega\, dt = \int_{t,\Gamma} \kappa \nabla \phi \cdot \boldsymbol{n}\, d\Gamma\, dt - \int_{t,\Omega} f'(\phi)\, d\Omega\, dt$$

Simplifying each term:

- $$\int_{t,\Omega} \frac{\partial \phi}{\partial t} d\Omega\, dt = \int_{\Omega} \left(\phi^{n+1} - \phi^{n}\right) d\Omega = \left(\phi_p^{n+1} - \phi_p^{n}\right) \Omega_p$$

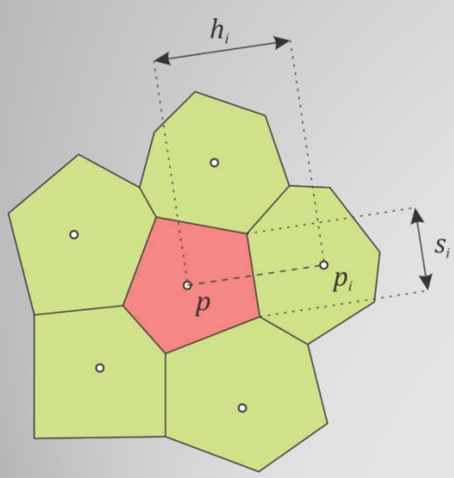

- $$\int_{t,\Gamma} \kappa \nabla \phi \cdot \boldsymbol{n}\, d\Gamma\, dt = \int_{t} \sum_{\mathrm{P}} \left[\kappa \nabla \phi^{n} \cdot \boldsymbol{n}\, s\right]_i dt = \left(\sum_{\mathrm{P}} \left[\left(\kappa \frac{\partial \phi^n}{\partial n} \right)_{p,p_i} s_i \right] \right) \Delta t = P_3$$

$$\left(\frac{\partial \phi^n}{\partial n} \right)_{p,p_i} = \frac{\phi_{p_i}^n - \phi_p^n}{h_i}$$

- $$\int_{t,\Omega} f'(\phi)\, d\Omega\, dt = \Omega_p \Delta t\, f'(\phi^n) = \Omega_p \Delta t \begin{cases} \phi_{i,j}^{n+1}\left(1-\phi_{i,j}^{n}\right) r\left(\phi_{i,j}^{n}\right) & \text{for } r\left(\phi_{i,j}^{n}\right) \le 0 \\ \phi_{i,j}^{n}\left(1-\phi_{i,j}^{n+1}\right) r\left(\phi_{i,j}^{n}\right) & \text{for } r\left(\phi_{i,j}^{n}\right) > 0 \end{cases}$$

CVT based finite volume method

Semi-implicit updating scheme:

$$\phi_{i,j}^{n+1} = \begin{cases} \dfrac{\Omega_p \phi_{i,j}^n + P_3}{\Omega_p \left(1 - \left(1 - \phi_{i,j}^n\right) r\left(\phi_{i,j}^n\right) \Delta t\right)}, & \text{for } r\left(\phi_{i,j}^n\right) \le 0 \\ \dfrac{\Omega_p \phi_{i,j}^n \left(1 + r\left(\phi_{i,j}^n\right) \Delta t\right) + P_3}{\Omega_p \left(1 + \phi_{i,j}^n r\left(\phi_{i,j}^n\right) \Delta t\right)}, & \text{for } r\left(\phi_{i,j}^n\right) > 0 \end{cases}$$

where,

$$r\left(\phi_{i,j}^n\right) = \phi_{i,j}^n - \frac{1}{2} - 30\eta \frac{\bar{J}'(\phi_{t1})}{\left\|\bar{J}'(\phi_{t1})\right\|} \phi_{i,j}^n \left(1 - \phi_{i,j}^n\right)$$

Implementation flow chart

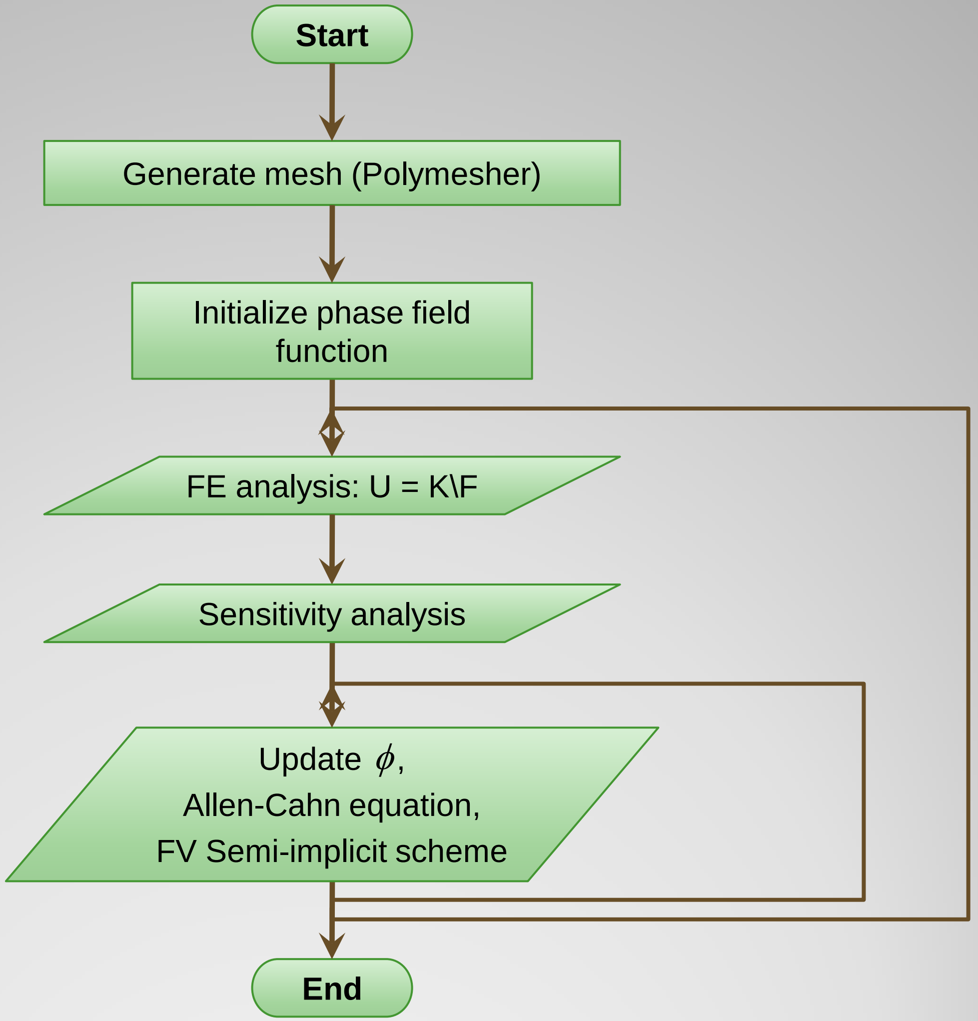

Numerical example 1

Cantilever beam problem

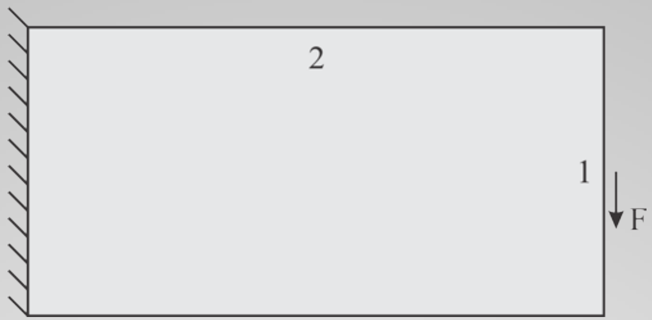

- Objective: Compliance minimization
- Domain size: 2x1 with 3200 polygonal elements
- FE iterations: 50
- For each FE iteration, 20 Allen-Cahn equation updates using CVT based FV method
- $\kappa = 10 \times 10^{-5}, \quad \eta = 10, \quad k_{\min} = 10^{-4}$

Numerical example 1

Cantilever beam problem

Polygonal Elements (3200)

Q4 Elements (80x40)

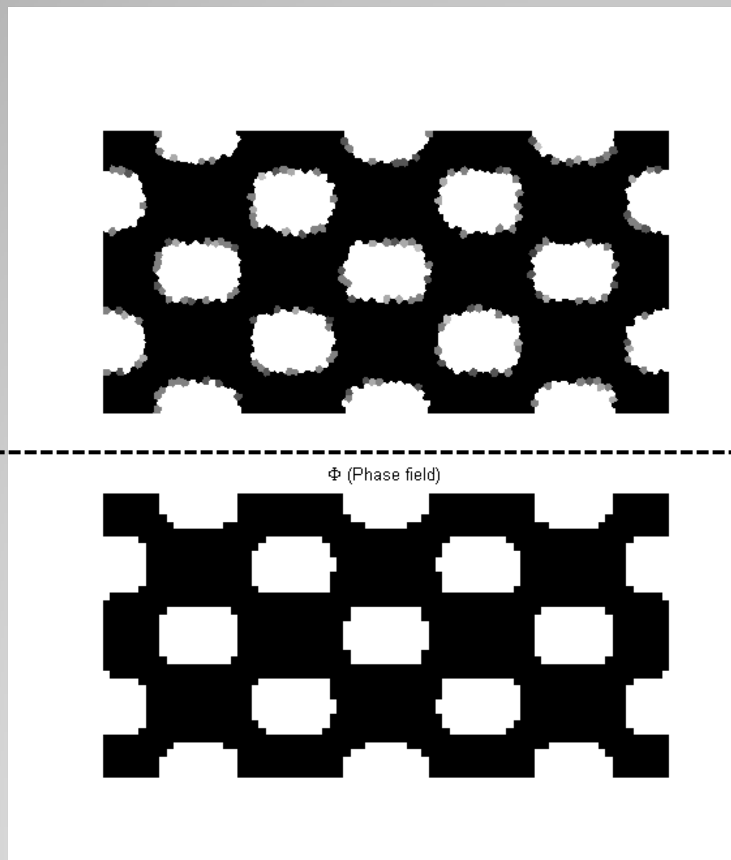

Initial guess

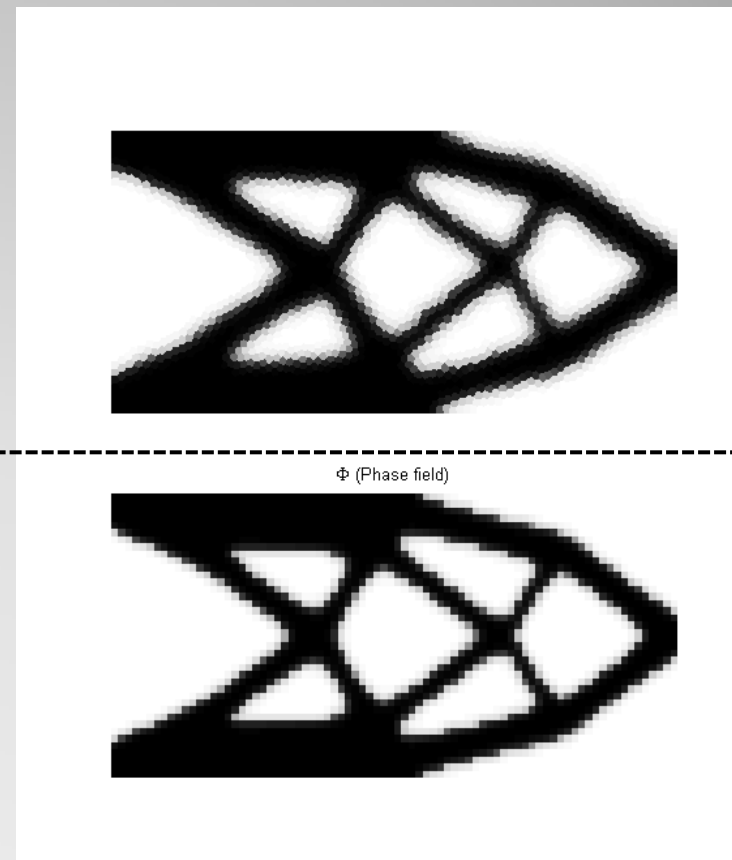

Topology after 50 iterations

Numerical example 2

Non-Cartesian domains

Cantilever beam problem on circular segment design domain

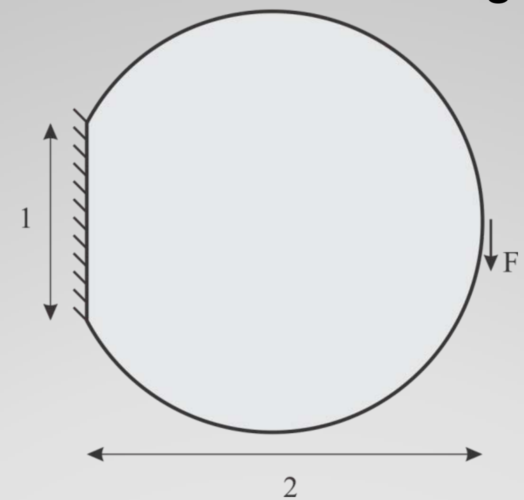

- Objective: Compliance minimization
- Domain size: 3000 polygonal elements
- FE iterations: 200
- For each FE iteration, 20 Allen-Cahn equation updates using CVT based FV method
- $\kappa = 10 \times 10^{-5}, \quad \eta = 10, \quad k_{\min} = 10^{-4}$

Numerical example 2

Non-Cartesian domains

Cantilever beam problem on circular segment design domain

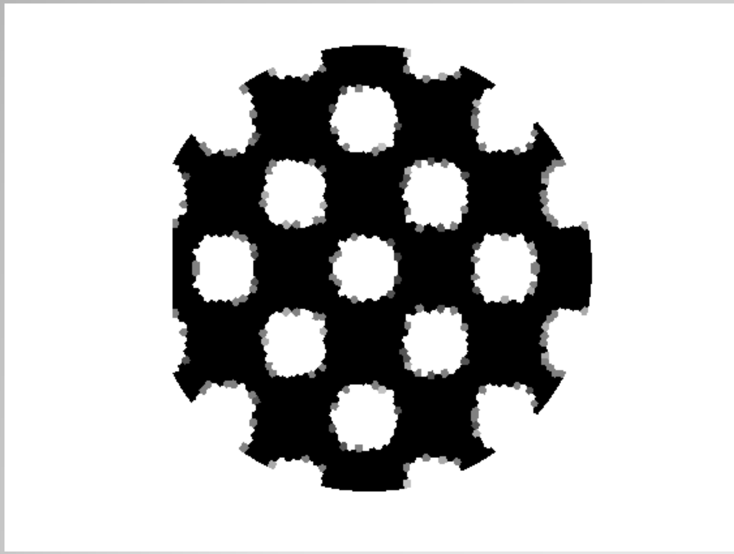

Initial guess

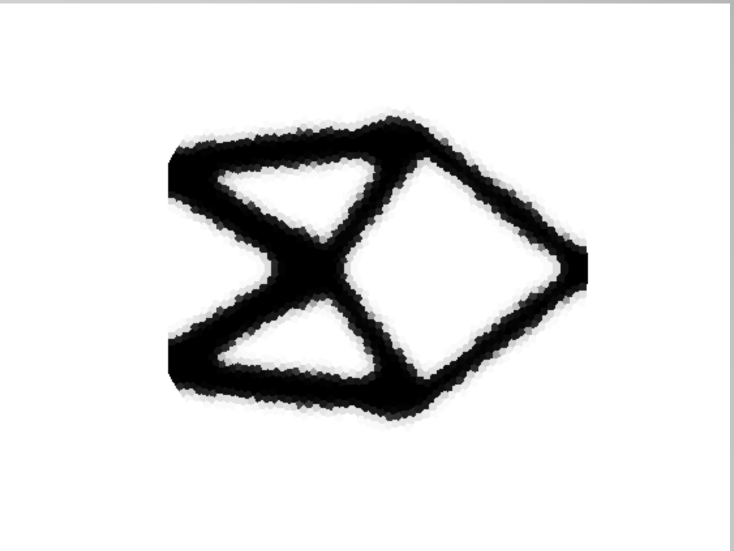

Topology after 200 iterations

Numerical example 3

Non-Cartesian domains

Bridge problem on semi-circular design domain

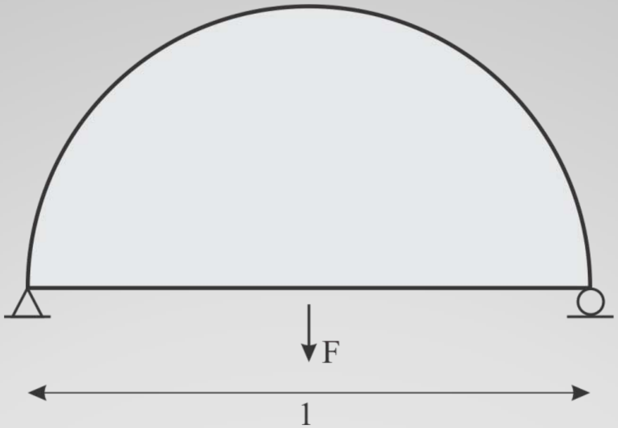

- Objective: Compliance minimization
- Domain size: 3840 polygonal elements
- FE iterations: 100
- For each FE iteration, 20 Allen-Cahn equation updates using CVT based FV method
- $\kappa = 10 \times 10^{-5}, \quad \eta = 10, \quad k_{\min} = 10^{-4}$

Numerical example 3

Non-Cartesian domains

Bridge problem on semi-circular design domain

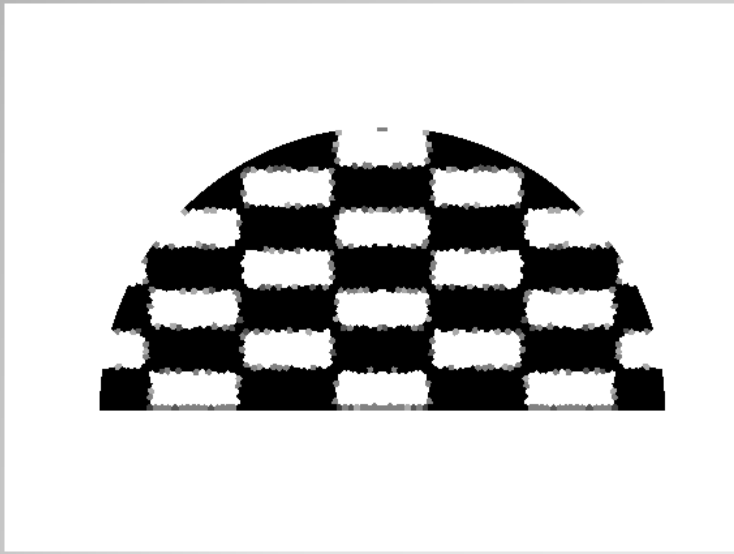

Initial guess

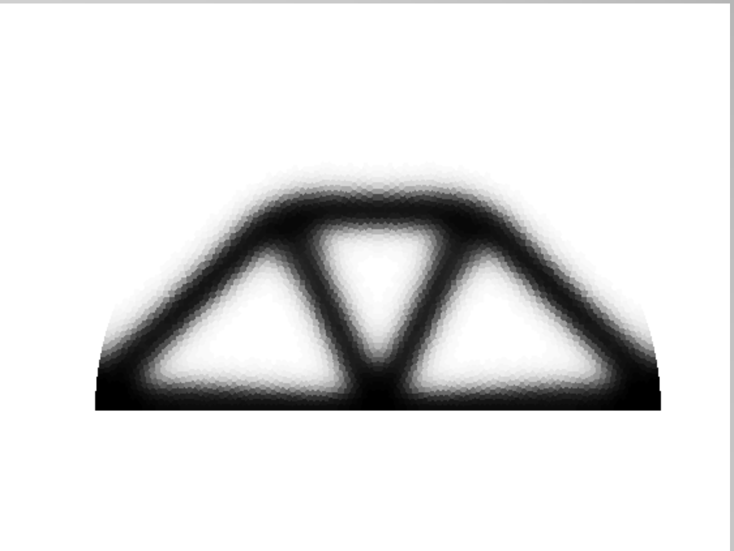

Topology after 100 iterations

Numerical example 4

<u>Non-Cartesian domains</u>

Doubly curved cantilever beam problem

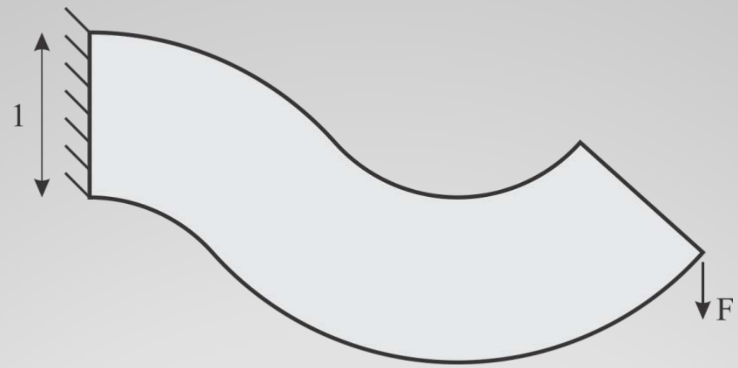

- <u>Objective</u>: Compliance minimization
- <u>Domain size</u>: 3200 polygonal elements
- <u>FE iterations</u>: 100
- For each FE iteration, 20 Allen-Cahn equation updates using CVT based FV method
- $\kappa = 10 \times 10^{-5}, \quad \eta = 10, \quad k_{\min} = 10^{-4}$

Numerical example 4

<u>Non-Cartesian domains</u>

Doubly curved cantilever beam problem

Numerical example 4

Non-Cartesian domains

Doubly curved cantilever beam problem

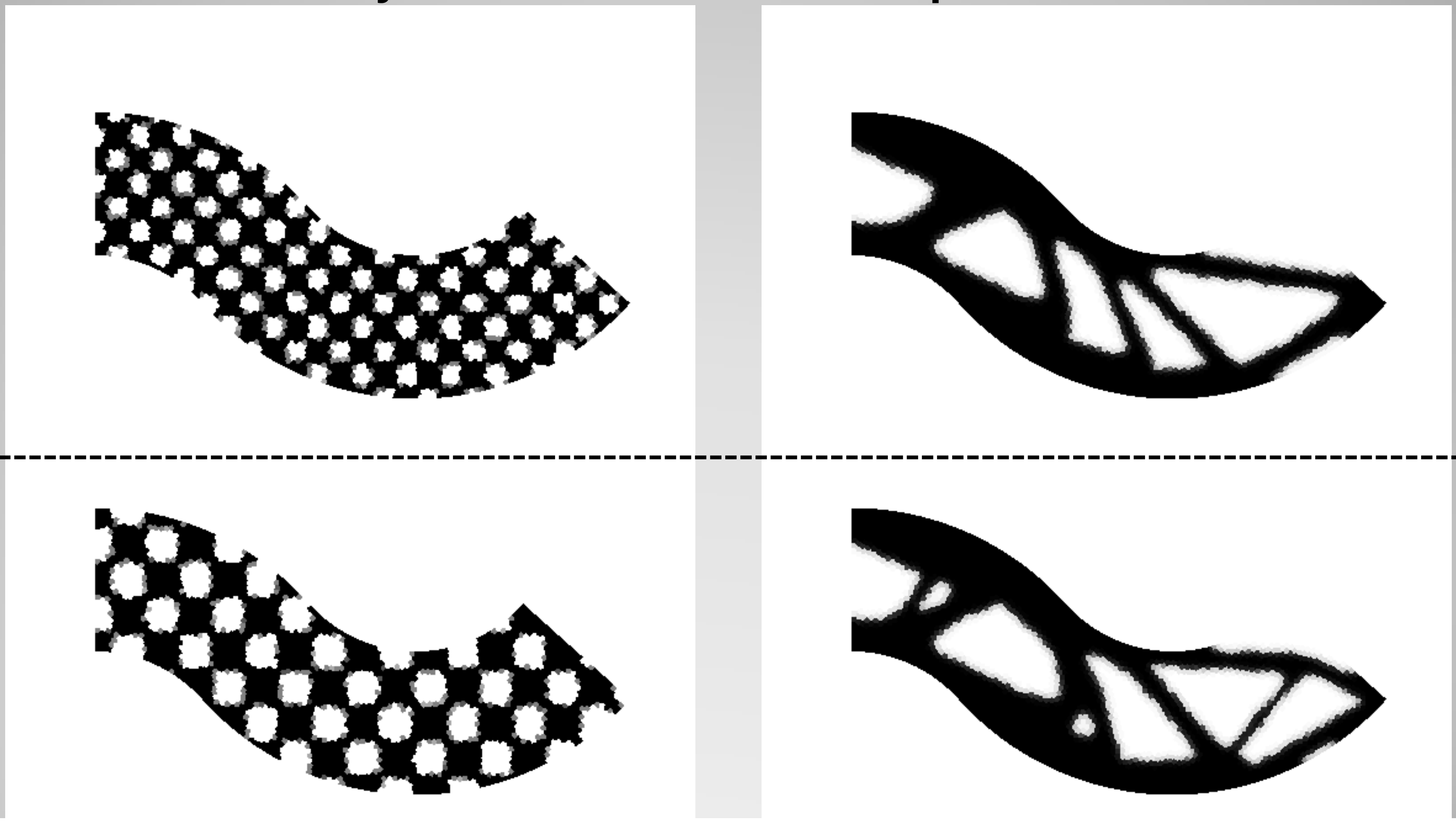

Initial guess

Topology after 100 iterations

Numerical example 5

Non-Cartesian domains

Inverter problem on circular segment design domain

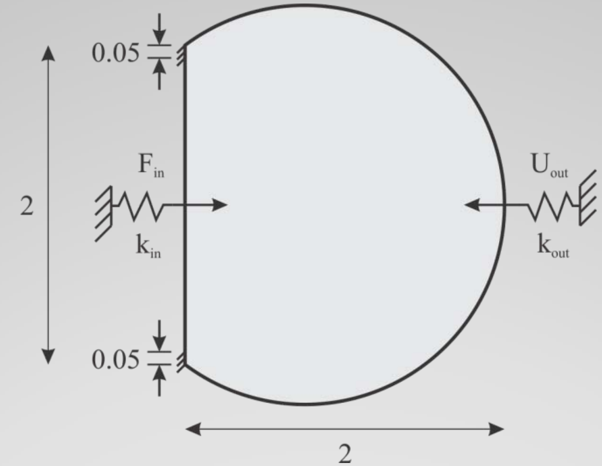

- Objective: Compliant mechanism
- Domain size: 6000 polygonal elements
- FE iterations: 300
- For each FE iteration, 20 Allen-Cahn equation updates using CVT based FV method
- $\kappa = 10\times10^{-5}, \quad \eta = 10, \quad k_{min} = 10^{-4}$

Numerical example 5

<u>Non-Cartesian domains</u>

Inverter problem on circular segment design domain

Numerical example 5

Non-Cartesian domains

Inverter problem on circular segment design domain

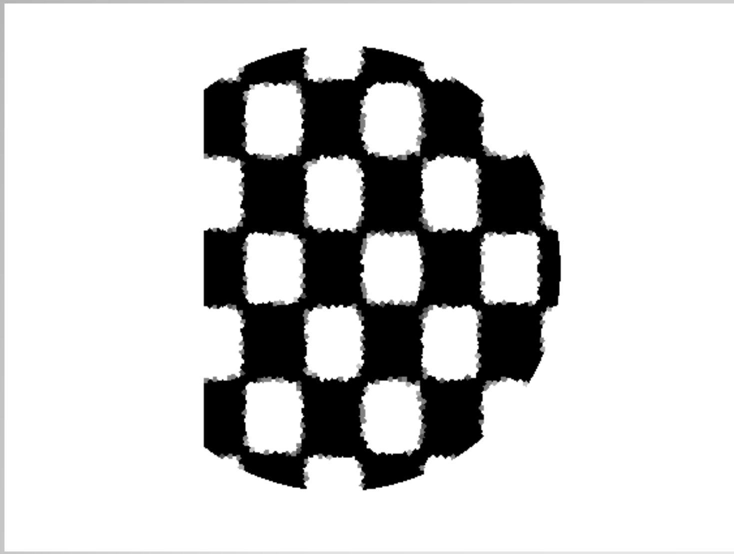

Initial guess

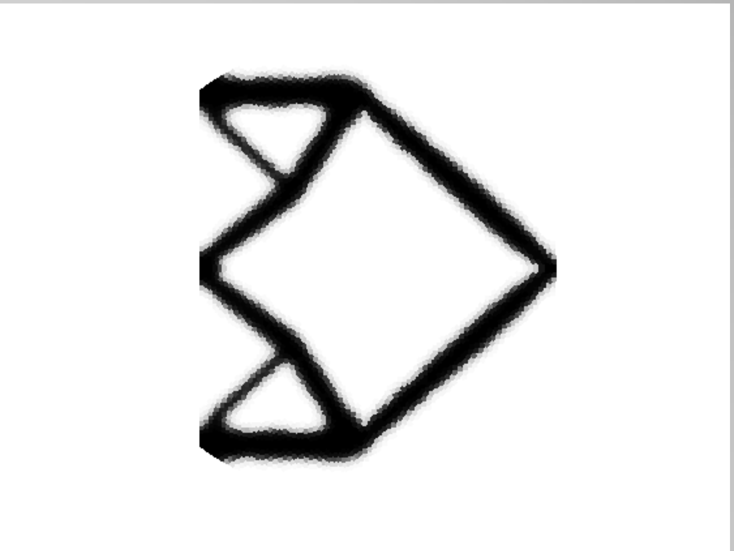

Topology after 300 iterations

Summary & Conclusions

- Implicit function-based phase field method using polygonal finite elements offers a general framework for topology optimization on arbitrary domains.
- Meshes based in simplex geometry such as quads/bricks or triangles/tetrahedra introduce intrinsic bias in standard FEM, but polygonal/polyhedral meshes do not.
- Polygonal/polyhedral meshes based on Voronoi tessellation not only remove numerical anomalies such as one-node connections and checkerboard pattern but also provide greater flexibility in discretizing non-Cartesian design domains.

Future extensions

Extension to 3D using polyhedral meshes

Courtesy: Stromberg et. al.

Phase field method with sharpness control of diffuse interfaces offer an attractive framework for phononic metamaterial cloaking design

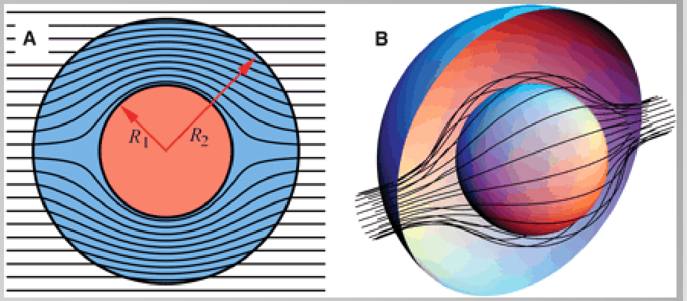

Courtesy: Pendry et. al., Science 312

Phase field method using polygonal meshes paves the way for medical engineering applications including craniofacial segmental bone replacement

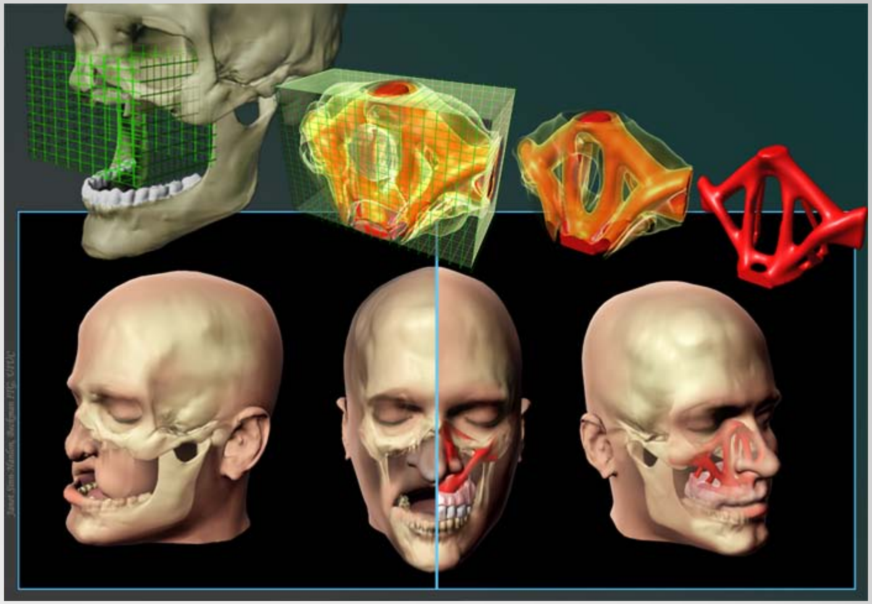

Sutradhar A, Paulino GH, Miller MJ, Nguyen TH (2010) Topology optimization for designing patient-specific large craniofacial segmental bone replacements. Proceedings of the National Academy of Sciences 107(30): 13222-13227

Thank You !